

Stress-Strain Curves of Sheet Material in High-Rate Forming Processes

S.Golovashchenko¹, V.Mamutov²

¹ Manufacturing & Processes Department, Ford Research & Advanced Engineering, USA

² Chair of Machines & Technology of Metal Forming, St.Petersburg Polytechnical University, Russia

Abstract

Electromagnetic forming technologies are based on high-voltage discharge of capacitors through the conductive coil. Two methods of testing and the results of dynamic coefficient k_d for aluminum alloys, copper, brass, steel, and some other materials are presented. The first method is based on expansion of rings machined from tubular blanks, which are designated for further stamping operations. The displacement of the ring was registered by using the light shading method. Parameters of the discharge electric current running through the electromagnetic coil were measured with a Rogowski gauge. The acceleration stage of the ring expansion process was used for more accurate calibration of the inductive gauge defining the parameters of electromagnetic pressure. Registering the kinematics of the ring during the inertial stage of the deformation process provided the information on dynamic behavior of the studied material.

The second method employed in this paper for dynamic yield stress measurement was based on transverse pulsed loading of a sheet sample clamped by its ends. Shapes of the samples during their deformation were photographed using a high-speed camera. The specifics of the sheet sample deformation under the pulsed transverse load are the following: the sample has near-trapezoidal shape; the middle part of the sample has almost the same velocity v_0 through the whole process; the angle between two inclined parts of the sample and the horizontal middle area γ has minor variation during the deformation process. In some cases, hybrid stamping processes including conventional forming on the press and final shape calibrating with pulsed forming technique require additional information about the influence of the static preliminary deformation of the sheet on dynamic yield stress. Experiments with different levels of material prestrain were conducted for this purpose.

Keywords:

Forming, Sheet, High Strain-Rate

1 Introduction

Electropulsed forming technologies are based on high-voltage discharge of capacitors through the conductive coil or between the electrodes in water. These processes generate high pressure on a sheet or tubular blank being formed, calibrated or assembled with other parts. The important benefits of pulsed technologies include low investment in one-sided dies [1], increased formability [2], reduced wrinkling and springback [3]. Material properties under high strain-rate deformation are the necessary input to analyze all pulsed stamping and joining operations.

Strain rates in pulsed electromagnetic forming and electrohydraulic forming of sheet material are usually within the following range $\dot{\varepsilon} \in [10^2-10^3] \text{ s}^{-1}$. This range significantly exceeds conventional tensile test conditions of $\dot{\varepsilon}_0 = 10^{-4} \text{ s}^{-1}$. Approximate information on dynamic stress-strain curves is especially important regarding the design stage of pulsed stamping processes. For example, for calibration of parts stamped from sheet metal or tubular blanks we need to estimate the required energy, choose the right duration of the pressure pulse, and design the calibration die appropriately to provide its sufficient durability. Each of these tasks requires preliminary data on material behavior under high strain rates. Later on this information can be corrected after conducting additional experiments with existing tools.

One of the possible approaches to this problem is based on the assumption that the average strain rate of the stamping process $\dot{\varepsilon}$ significantly exceeds the strain rate of the static test $\dot{\varepsilon}_0$. If this assumption is valid it is possible to represent the stress-strain rate function with reasonable accuracy based on the static curve $\sigma_s(\varepsilon_i, \dot{\varepsilon}_0)$ multiplied by some dynamic functional $k(\varepsilon_i, \dot{\varepsilon})$:

$$\sigma_s = k(\varepsilon_i, \dot{\varepsilon}) \sigma_s(\varepsilon_i, \dot{\varepsilon}_0) \quad (1)$$

For simplicity the functional can be replaced by some dynamic coefficient k^d valid in a certain range of strain rates. The dynamic coefficient can be represented as a power function

$$k = \left(\frac{\dot{\varepsilon}}{\dot{\varepsilon}_0} \right)^m \quad (2)$$

If the strain rate value $\dot{\varepsilon}$ exceeds the value of $\dot{\varepsilon}_0$ in several orders of magnitude, the functional $k(\varepsilon_i, \dot{\varepsilon})$ can be replaced by the integral dynamic coefficient k^d [4]. Variation of the dynamic coefficient for most part of some high-rate stamping process can be relatively small. Usually the strain rate of the high-speed stamping processes varies within one or two orders of magnitude.

$$\frac{1}{T} \int_0^T \varepsilon_i(t) \cdot dt \in [\dot{\varepsilon}_{max}, \dot{\varepsilon}_{min}], \quad \frac{\dot{\varepsilon}_{max}}{\dot{\varepsilon}_{min}} < 10^1 \dots 10^2 \quad (3)$$

where T is duration of the stamping process. Taking into account that the parameter m in (2) for majority of metals is a small value, an average dynamic coefficient can be used instead of the function of strain-rate hardening for each material in some limited interval of strain rates.

$$k^d = \left[\frac{(\dot{\varepsilon}_{min} + \dot{\varepsilon}_{max})}{(2\dot{\varepsilon}_0)} \right]^m \in [k_{min}^d, k_{max}^d] \quad (4)$$

On a design stage of the stamping processes such simplification is valid because for the majority of experimental methods defining the parameters of a dynamic stress-strain curve the following inequity is valid:

$$2 \frac{(k_{max}^d - k_{min}^d)}{(k_{max}^d + k_{min}^d)} < \gamma \quad (5)$$

where γ is the relative error of the experimental results.

Several methods of defining dynamic stress-strain curves of metals are known in the literature. One of the simplest is the method of expansion of rings, which allows to create the stress state in the sample close to the uniaxial tension similar to a standard test [3,5]. Effects of waves propagation do not create significant distortions; therefore, the stress and strain distributions are close to being uniform. The other well-known method is based on the transverse impact on the sheet metal, where the speed of the plastic wave propagation is the most important factor defining the dynamic yield stress [6,7,8]. In many cases, high-speed forming is used after the conventional forming. Therefore, some adjustments of this method allowing the study of the effect of preliminary deformation on the dynamic yield stress [9] are beneficial. Employment of various methods for the same material provides more reliable data as to their dynamic behavior. It also helps to calibrate the technique of measurements and data processing.

2 Study of dynamic behavior of metals using expansion of rings

The schematic of the experimental technique used in this paragraph is shown in Figure 1.

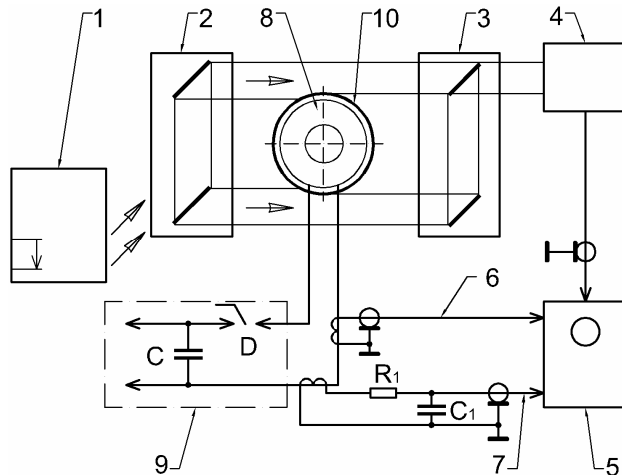


Figure 1: Schematic of the experimental device to study the dynamic yield stress by registering the dynamics of the ring expansion: 1 - optical laser, 2 - block of beams formation, 3 - summation block, 4 - receiver based upon the photo-electronic multiplier, 5 - oscilloscope, 6 - Rogowski gauge, triggering the oscilloscope, 7 - Rogowski gauge with integration RC contour for measurement of the discharge current, 8 - coil, 9 - electromagnetic forming machine, 10 - ring to be expanded

A beam from the optical laser 1 is transformed into two identical parallel beams of rectangular cross-section and rather uniform distribution of light intensity using the block of beams formation 2. The thickness and width of the beam as well as the distance between two beams can be tuned according to the dimensions of the ring used in experimental studies. The summation block 3 adds both beams and directs them to a receiver 4 based on a photo electronic multiplier. The receiver is equipped with the narrow range light filters, which allow to separate the actual signal from the general light. The receiver was mounted inside the metal box in order to protect it from the electromagnetic noise. The electromagnetic coil 8 is positioned inside the ring 10, which is being accelerated during the high-voltage discharge of electric capacitors of the electromagnetic forming machine 9 through the coil. During the expansion of the ring driven by internal electromagnetic pressure, the wall of the ring is shading the beams of the laser. This results in a changing of the luminous flux coming to the receiver and registered by the oscilloscope 5. The initiation of the oscilloscope was carried out by a signal from Rogowski gauge 6. The signal from the other Rogowski gauge 7 was integrated using a R-C contour and also registered by the oscilloscope. This signal was necessary to define the moment when the discharge of the electromagnetic forming machine is completed. From that moment on, further deformation of the ring is purely inertial.

The experiments were conducted using an electromagnetic forming machine with the following parameters: capacitance - 215 μF , maximum charging voltage - 20 kV; frequency of the machine dictated by its L-C combination - 24 kHz. The rings had the following dimensions: external diameter - 44 mm; width - 3 mm; thickness - 1 mm. Copper samples were annealed in vacuum at a temperature of 560°C for one hour. The multi-turn coil machined from a brass bar was press-fit over the micarta internal mandrel. The absence of error signals was checked by discharging capacitors through the coil without placing a ring and having the signal from the light receiver constant during the discharge process and also by switching on and off the light in the laboratory.

The simplest static linearity of the displacement measuring system can be checked by placing a ring of a larger diameter than the samples used in the expansion experiment and then moving this larger ring to different sides as a rigid body, shading different light beams. If the system is linear the signal of the ring displacement, corresponding to the ring outer diameter, should be the same. The dynamic linearity of the system was checked by an optical chopper disc rotated at a high speed. In order to make the pressure pulse shorter, the additional active resistance was connected in series with the coil. The value of this resistance was adjusted to provide an aperiodic discharge of capacitors. The example of oscillograms from the photo electronic multiplier, proportional to the radial displacement of the ring, and from the Rogowski gauge, proportional to the discharge electric current, are shown in Figure 2.

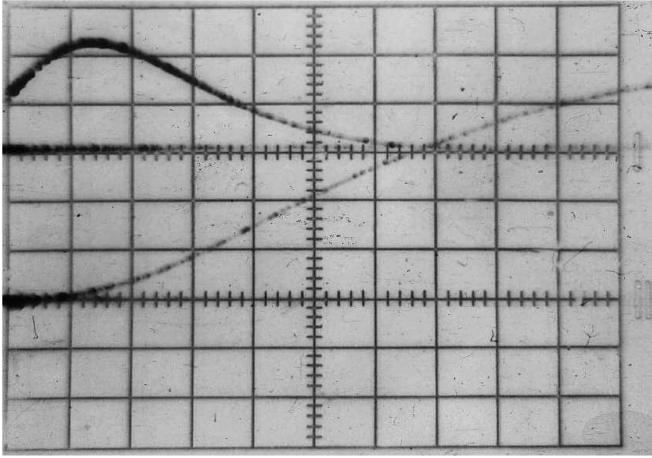
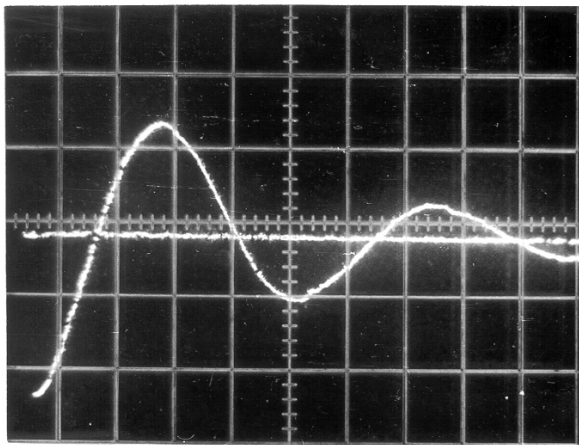
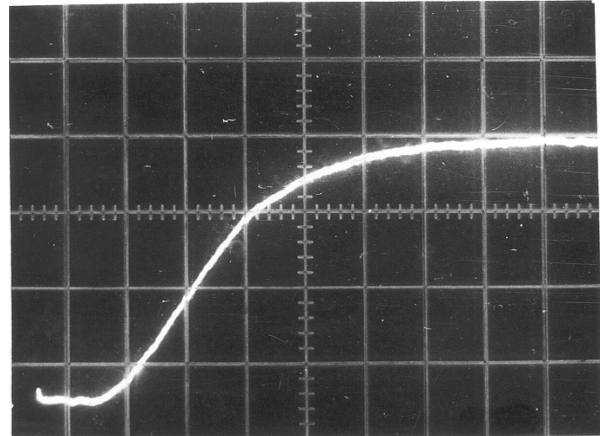


Figure 2: Example of the oscillogram combining the radial displacement of the ring during its expansion combined with discharge current vs time. The scale along the horizontal axis was 10 μsec. Maximum displacement of the ring was 3.4 mm



a



b

Figure.3: Examples of oscillograms of the induced electromotive force in the inductive gauge (a) and displacement of the ring being expanded (b). The scale along the horizontal axis is 20 μsec

In order to define the dynamic behavior of studied materials, we used the integral energy conservation law. The dynamic coefficient k^d was defined by the following relationship:

$$k^d = \frac{\sigma_s^d}{\sigma_s^s} = \frac{\int_{\varepsilon_i \in [\varepsilon_{i1}, \varepsilon_{i2}]} \sigma_s^d(\varepsilon_i) d\varepsilon_i}{\int_{\varepsilon_i \in [\varepsilon_{i1}, \varepsilon_{i2}]} \sigma_s^s(\varepsilon_i) d\varepsilon_i} \quad (6)$$

Where σ_s^d and σ_s^s are the average values of dynamic and static yield stresses in the given interval of strain intensity variation $[\varepsilon_{i1}, \varepsilon_{i2}]$ corresponding to the conditions of the experiment. For the ring expansion process, the circumferential deformation is equal to the strain intensity and can be defined as:

$$\varepsilon_1 = \varepsilon_i = \ln\left(\frac{r}{r_0}\right) \quad (7)$$

where r_0 and r are the original and current radii of the ring during the deformation process. The data from the oscillograms were processed during the interval of time $t \in [t_1, t_2]$ after the discharge of capacitors was completed and no electromagnetic pressure was applied to the ring. During this interval the ring is moving due to its mass inertia. The interval boundaries are defined in the following way: $t_1 > t_p$, where t_p is time when the pressure pulse was completed; $t_2 < t_{\text{end}}$, where t_{end} is the time when the plastic deformation process was completed and the ring stopped. For this interval, the energy conservation law can be used in the following form:

$$\frac{\rho[\dot{r}^2(t_1) - \dot{r}^2(t_2)]}{2} = \int_{\varepsilon_i(t_1)}^{\varepsilon_i(t_2)} \sigma_s^d(\varepsilon_i) d\varepsilon_i \quad (8)$$

where ρ is the mass density of the ring material; $\dot{r}^2(t_1)$, $\dot{r}^2(t_2)$ - radial velocity of the ring corresponding to the moments t_1 and t_2 . Having known the parameters of the static stress-strain curve, the dynamic coefficient can be estimated from the following equation:

$$k^d = \frac{\rho[\dot{r}^2(t_1) - \dot{r}^2(t_2)]}{2 \int_{\varepsilon_i(t_1)}^{\varepsilon_i(t_2)} \sigma_s^d(\varepsilon_i) d\varepsilon_i} \quad (9)$$

The values of velocities $\dot{r}(t_1)$ and $\dot{r}(t_2)$ were defined by numerical differentiation of the curve of radial displacement of the ring.

For the annealed copper M1 the average dynamic coefficient was obtained as $k^d = 1.35 \pm 0.20$. The averaging was conducted in the interval of strain rates of $\dot{\varepsilon} \in [0.8, 1.6] \cdot 10^3 \text{ s}^{-1}$ and the range of strains $\varepsilon_i \in [0.05, 0.20]$.

The described approach offers the very important advantage of excluding the uncertainty of registration of the pulsed load. This solution may not be feasible for materials with low ductility where the expansion of the ring is limited by its splitting, or in case of using the medium voltage electromagnetic forming machines (up to 5 - 6 kV of charging limit) and the coil with multiple turns with rather slow pressure pulse. In both of these cases, the electromagnetic pressure affects the deformation of the ring almost through the whole deformation process and equation (8) is not valid. The employment of the Rogowski gauge can also bring some averaging of the electromagnetic pressure along the coil axis. In this case a possible solution lies in installing the inductive gauge in the space between the coil and the ring, so we can register the applied pressure more accurately. It should be specified that the gauge has to be electrically insulated from both the coil and the ring. To satisfy this requirement, we mounted the inductive gauge outside the multiturn cylindrical coil in between the layers of the glass tape, covered by epoxy. After solidification the external surface of such an insulation was machined to fit accurately inside the ring. The inductive gauge was positioned approximately in the middle of the coil along its z-axis in order to get a uniform distribution of the electromagnetic pressure. The electromotive force $E(t)$ generated inside the inductive gauge was registered by the oscilloscope parallel to the radial displacement of the ring. According to [10] it can be represented as

$$E(t) = \frac{d\Phi}{dt} = -\mu_0 S_{\text{effective}} \frac{dH(t)}{dt} \quad (10)$$

where $H(t) = H_0 e^{-\delta t} \sin \omega t$ t – time; μ_0 – magnetic permeability of vacuum; δ, ω – the damping coefficient and circular frequency; $S_{\text{effective}}$ is the geometric characteristic of the inductive gauge, which was defined by a separate test of the ring expansion made from annealed aluminum. The deformation of the thin ring driven by pulsed electromagnetic pressure can be defined by a simple equation:

$$p_0 e^{-2\delta t} \sin^2 \omega t = \frac{\sigma_s^s}{R} + \rho s \frac{d^2 R}{dt^2} \quad (11)$$

where p_0 is the pressure amplitude at $t = 0$; σ_s is current material yield stress; ρ is material density; s and R are current thickness and radius of the ring, changing during the deformation process.

In the beginning of the process, during the ring quick acceleration stage, the first term in the right part of the equation can be found using a dynamic stress-strain curve of a known material or known dynamic coefficient and static curve. During this stage, the second term in the right side of the equation (11) clearly dominates over the first term, representing the energy dissipation through plastic deformation. Based on this consideration, the inductive gauge was calibrated during this stage and then used for further analysis of the material behavior. It was conducted by solving the equation (11) relatively the unknown value of σ_s at every time step. From the first glance, it looks very attractive to differentiate twice the function $R(t)$ known from the experiment and find the unknown σ_s . However, some errors of registration $R(t)$ can make the result inaccurate. Instead of that, we used the implicit procedure of integration adjusting σ_s to satisfy the $R(t)$ curve and then smoothing the obtained results.

The technique described in this paragraph has some drawbacks including rather difficult tuning of the measuring system. It also has some limitation regarding electrical conductivity of the material being tested. For these reasons, the data obtained with this method was mostly used for an estimation of the results obtained with the transverse impact method.

3 Study of the dynamic behavior of metals using the transverse impact method

The method of transverse impact is based upon the specifics of the plastic waves propagation inside thin strip of metal sheet clamped by its edges. During the deformation process the strip has the shape of trapezoid, while both the velocity v_0 of the central part of the strip and the angle γ between inclined and horizontal parts of the strip are almost constant through the whole process. Experimental data on v_0 and γ allows the calculation of the dynamic yield stress [8]

$$\sigma_s^d = \rho \left[\frac{v_0}{\tan(\gamma)} \right]^2 \quad (12)$$

Having defined the values of both dynamic and static yield stresses σ_s^d and σ_s^s , it is easy to find the dynamic coefficient k^d . The schematic of the measuring device is shown in Figure 4.

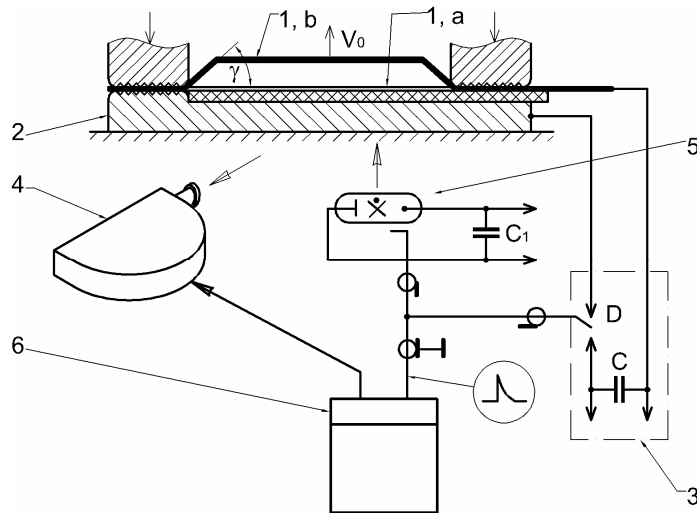


Figure 4: Schematic of measurement of the strip kinematics after transverse pulsed loading with electromagnetic field (1 – sample being tested, a – in original position; b – during the deformation process; 2 – fixture for clamping the sample; 3 – electromagnetic forming machine; 4 – high-rate photo camera; 5 – block of pulsed light generation; 6 – control desk of the high-rate camera)

The discharge current from the electromagnetic forming machine 3 is running through the supporting copper plate 2 and then through the sample 1, clamped by its edges. Driven by the pulse of electromagnetic pressure, the sample 1 quickly gains its initial speed and then goes through the deformation process. Photographing of the sample deformation history was conducted by a high-speed photo-registrator in reflected light of the flash lamp 5. Synchronization of the flash light, the deformation process, and its photo registration was conducted employing the special synchronization pulse from photo-registrator 6.

The samples for testing were fabricated from metal sheets 0.5 – 0.8 mm thick, 10 mm wide, and 160 mm long. The pulsed load generated by a pulsed electromagnetic field has some limitations mostly related to material electric conductivity. Due to this fact, copper, aluminum and their alloys are good candidates for such type of loading. In order to test samples from materials with significantly lower conductivity, the samples were coated by a layer of copper having the thickness of 0.003 – 0.05 mm. The described coating significantly improves the conditions for using pulsed electromagnetic fields as a source of impact transverse loads without adding any significant distortion into the experimental data. The examples of pictures illustrating the sample shape during the deformation process are shown in Figure 4.

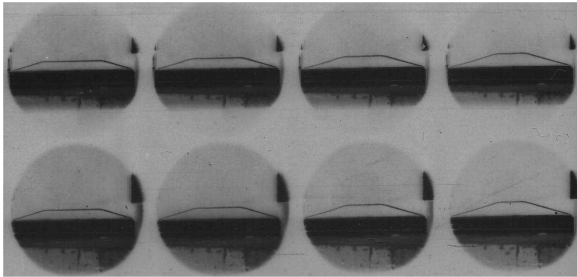


Figure 5: Example of high-rate photo registration of sheet samples after the transverse pulsed loading (the rate of photographing is 62500 pictures/ second; the pictures are organized in a way that the top row includes odd numbers and the bottom row includes even numbers of pictures; the material of samples is copper M1)

In order to study the effect of preliminary deformation and work hardening on the dynamic yield stress of tested metal, a special device was employed enabling the variation of the preliminary deformation.

4 Experimental results

The experimental data on testing the variety of metals is listed in Table 1. Each set of parameters was repeated from seven to ten times. Rounded up to the second digit, the number of trust interval was defined using the Student criterion and 95% of trust probability.

N	Material	Method of testing ¹	Preliminary deformation	Static yield stress, MPa	Dynamic coefficient k^d
1	Duralumin D16AM	2	0	127	1.65±0.15
2	Aluminum alloy, AMnM	2	0	56	1.30±0.20
3	Aluminum, AD1	2	0	90	1.35±0.10
4	Nickel	2	0	180	1.40±0.15
5	Molybdenum	2	0	1040	1.10±0.10
6	Niobium	2	0	416	1.10±0.05
7	Stainless steel	2	0	233	1.10±0.10
8	High Strength Steel	2	0	290	1.25±0.10
9	Brass	2	0	110	1.25±0.10
10	Copper, M1	1	0	102	1.35±0.20
11	Copper, M1	2,3	0	102	1.40±0.20
12	Copper, M1	3	0.09	183	1.30±0.15
13	Copper, M1	3	0.17	222	1.25±0.20
14	Mild steel, 08	2,3	0	185	1.30±0.15
15	Mild steel, 08	3	0.065	260	1.20±0.15
16	Mild steel, 08	3	0.125	310	1.15±0.10
17	Mild steel, 08	3	0.185	342	1.10±0.10

¹ 1 = pulsed expansion of rings; 2 = transverse impact; 3 = transverse impact with possible variation of the prestrain deformation

Table 1

5 Conclusions

Analysis of experimental data indicates that for testing samples of copper the method of ring expansion and the method of transverse impact provide sufficiently close results within the range of statistical deviation.

The increase of yield stress due to high strain-rate of testing for the majority of metals used in stamping can vary from several percents to 65%, which has to be considered on the design stage of the technological process of high-speed stamping.

References

- [1] *Wilson F.W., ed.*: American Society of Tool and Manufacturing Engineers: High Velocity Forming of Metals (Prentice-Hall, Inc, Englewood Cliffs, N.J. 1964).
- [2] *Golovashchenko, S.; Mamutov, V.; Dmitriev, V.; Sherman, A.*: Formability of sheet metal with pulsed electromagnetic and electrohydraulic technologies, Proceedings of TMS symposium "Aluminum-2003," San-Diego, 2003, p.99-110.
- [3] *Golovashchenko S.*: Numerical and experimental results on pulsed tubes calibration, Proceedings of a 1999 TMS Symposium "Sheet Metal Forming Technology", San-Diego, 1999, p.117-127.
- [4] *Vagin, V.; Zdor G.; Mamutov V.*: Methods of analysis of high-rate deforming of metals, Minsk, 1990, 207p. –In Russian.
- [5] *Lopatin, A.*: Development of dynamic stress-strain diagrams by using tubular samples," Pulsed Forming of Metals. Issue N2, Charkov, 1970, p.128-136. –In Russian.
- [6] *Rahmatulin, H; Demyanov, Yu*: Strength under Intensive Short-Duration Loads, Moscow, 1961, 399 p. - In Russian.
- [7] *Shcheglov, B.; Vlasov B.*: Study of Plastic Deformation of Thin Sheets under Dynamic Loading, Mechanical Engineering, 1972, N6, p.85-90. -In Russian.
- [8] *Grushevskiy, A.*: Propagation of waves in Thin Strip and Study of Dynamic Yield Stress of Sheet Metals in Pulsed Stamping, Forging and Stamping Production, 1967, N8, p.21-25. – In Russian.
- [9] *USSR Patent 926567: Bogoyavlenskiy, K.; Mamutov, V., Oreshenkov, A.; Perezhogin, A.*: The Device for Study of Dynamic Yield Stress for Sheet Metals. - In Russian.
- [10] *Piekara, A.; Malecki, J.*: On a method of producing strong magnetic fields of short duration, Acta Physica Polonica. - 1956.-V.15, N4.-p.381-388.